Computing moments of objects enclosed by piecewise polynomial surfaces

Carlos Gonzalez-Ochoa Scott McCammon Jörg Peters

February 3, 1998

Abstract

Combining a polynomial free-form surface representation with Gauss' divergence theorem allows efficient and exact calculation of the moments of the enclosed object. For example, for a cubic representation, volume, center of mass and the inertia tensor can be computed in seconds even for complex objects with several thousand patches while changes due to local modification of the surface geometry can be computed in real time as feedback for animation or design. Speed and simplicity of the approach allow solving the inverse problem of modelling to match prescribed moments.

1 Introduction

Realistic animation and geometric design must both pay close attention to the physics implied by the first moments, the volume, center of mass and inertia frame, of the objects they manipulate. A jug whose fill level is inconsistent with the amount of water filled into it, or one that does not topple over when the projection of the center of mass moves outside the support, puzzles and distracts the viewer and can lead to disaster when unobserved in engineering design. While animators and designers often have an excellent intuitive grasp of the approximate physics implied by shape, the immediate and exact feedback from a tool like the one developed below can save the user both time and energy. Real time visual feedback and visualization of moments and the solution of simple inverse problems help identifying critical points in the moment distribution.

The key to fast and exact computation of moments of smooth free-form surfaces is to combine the advantages of a low-degree polynomial surface representation with Gauss' divergence theorem. Section 2 reviews how the well-known divergence theorem reduces the moment computation for piecewise polynomial surfaces to integrating related polynomials. Section 3 collects criteria on the surface representation that allow efficient application of this fact. For free-form surfacing, C^1-surface splines [15] match the bill and are used as a concrete representation of free-form manifolds in the following sections. Section 4 discusses the details of the evaluation of the surface integrals as simple averages of the coefficients and gives an operations count. In Section 5, we measure and visualize moments and in Section 6 we model geometry to match moments. Section 7 lists extensions and more applications ahead.

1.1 Prior work

The engineering literature is rich in applications of moments and algorithms for computing moments based on cellular, piecewise constant, or polyhedral, piecewise linear, *approximations* of the object ([11], [12], [2], the `massprop` command in the ACIS solid modeler), of its surface ([13],[14]), of the divergence theorem [25], or the associated integrals [24]. For example, [10] uses a subtle non-uniform extrapolation scheme which requires exact arithmetic to approximately evaluate moments.

While appropriate for non-polynomial or non-linearly trimmed surface representations, approximations are inappropriate, namely less efficient or accurate, for objects enclosed by standard polynomial patches, such as polynomial B-splines. The approximations obscure the fact that the *moment computation requires no evaluation of rational integrals or approximation of surface area*. The paper highlights this fact by combining a simple surface representation with classical formulas and thus illustrating the direct and exact computation of the first moments of smooth (and non-smooth) polynomial free-form surfaces of arbitrary patch layout and topological genus.

2 The elegant divergence theorem

Applied by Gauss in 1813, the well-known divergence theorem (see e.g. [21] 10.51), relates a volume integral to an integral over the surface. Given a map $\mathbf{f} : R^n \mapsto R^3$, its divergence $\nabla \cdot \mathbf{f} = \sum \frac{\partial}{\partial x_i} f_i$ and its normal component $\mathbf{f} \cdot N = \sum f_i N_i$, the theorem states that

$$\int_V \nabla \cdot \mathbf{f} \; dV = \int_S \mathbf{f} \cdot N \; dS$$

i.e. that the integral of the divergence of $\mathbf{f}$ over the volume V equals the integral of the normal component over the surface S of V.

To apply the theorem to moment calculations denote the parametrization of the surface S by

$$\mathbf{x}(\mathbf{u}) = [x, y, z](u, v) = \begin{pmatrix} x(u,v) \\ y(u,v) \\ z(u,v) \end{pmatrix},$$

and the domain of $\mathbf{x}$ by U, i.e. $(u, v) \in U$. The surface normal is the vector $N = \mathbf{n}/|\mathbf{n}|$ where

$$\mathbf{n} := \frac{\partial \mathbf{x}}{\partial u} \wedge \frac{\partial \mathbf{x}}{\partial v} = \begin{pmatrix} \frac{\partial y}{\partial u}\frac{\partial z}{\partial v} - \frac{\partial y}{\partial v}\frac{\partial z}{\partial u} \\ \frac{\partial z}{\partial u}\frac{\partial x}{\partial v} - \frac{\partial z}{\partial v}\frac{\partial x}{\partial u} \\ \frac{\partial x}{\partial u}\frac{\partial y}{\partial v} - \frac{\partial x}{\partial v}\frac{\partial y}{\partial u} \end{pmatrix}.$$

The crucial observation is that by change of variable

$$\int_S dS = \int_U |\mathbf{n}| \; dudv.$$

That is, the area element $|\mathbf{n}|$ is the inverse of the normalization factor of the normal direction so that

$$\begin{aligned} \int_V \nabla \cdot \mathbf{f} \; dV &= \int_S \mathbf{f} \cdot \mathbf{n}/|\mathbf{n}| \; dS \\ &= \int_U \mathbf{f} \cdot \mathbf{n} \; dudv \end{aligned}$$

If both $\mathbf{f}$ and $\mathbf{x}$ are polynomial the integrand is polynomial; and if U is a simple domain, say a triangle or square, then it is clear, and made precise in Section 4, that the integral can be determined efficiently, explicitly and exactly. This remains true if the parametrization $\mathbf{x}$ of S consists of patches $\mathbf{x}^i$ and U is the union of the patch domains U^i:

$$\int_U \mathbf{f} \cdot \mathbf{n} \; dudv = \sum_i \int_{U^i} \mathbf{f} \cdot \mathbf{n}^i \; du^i dv^i.$$

We now consider specific choices of $\mathbf{f}$ that allow us to determine the first three moments of a solid with uniform mass distribution. It is efficient to choose $\mathbf{f} = [0, 0, f_3]$ so that we need to compute only

$$n_3 = \frac{\partial x}{\partial u}\frac{\partial y}{\partial v} - \frac{\partial x}{\partial v}\frac{\partial y}{\partial u}.$$

The zeroth moment, $\mathcal{M}_0 = \int_V dV$, measures the volume enclosed by S. With $f_3 = z$,

$$\boxed{\mathcal{M}_0 \;\; = \int_U z \; n_3 \; dudv.}$$

The first moments $\mathcal{M}_i = \int_V x_i dV$ represent the components of the center of mass. Choosing f_3 as xz, yz and $z^2/2$ respectively yields

$$\boxed{\begin{array}{ll} \mathcal{M}_1 & = \int_U xz \quad n_3 \; dudv \\ \mathcal{M}_2 & = \int_U yz \quad n_3 \; dudv \\ \mathcal{M}_3 & = \int_U z^2/2 \; n_3 \; dudv \end{array}}$$

The second moments yield the components of the inertia tensor

$$\mathcal{I} = \begin{bmatrix} \int(x_2^2+x_3^2)dV & \int x_1 x_2 dV & \int x_1 x_3 dV \\ \int x_2 x_1 dV & \int(x_1^2+x_3^2)dV & \int x_2 x_3 dV \\ \int x_3 x_1 dV & \int x_3 x_2 dV & \int(x_1^2+x_2^2)dV \end{bmatrix}.$$

We list $\mathcal{M}_{ij} = \int_V x_i x_j dV$.

$$\begin{aligned}
\mathcal{M}_{11} &= \int_U x^2 z \quad n_3 \, dudv \\
\mathcal{M}_{12} &= \int_U xyz \quad n_3 \, dudv \\
\mathcal{M}_{13} &= \int_U xz^2/2 \, n_3 \, dudv \\
\mathcal{M}_{22} &= \int_U y^2 z \quad n_3 \, dudv \\
\mathcal{M}_{23} &= \int_U yz^2/2 \, n_3 \, dudv \\
\mathcal{M}_{33} &= \int_U z^3/3 \quad n_3 \, dudv
\end{aligned}$$

The above formulas assume that the volume has homogeneous density. If this is not the case but the anti-derivative of the moment-weighted mass distribution $\rho(x, y, z)$ is known, f_3 can be chosen so that similar formulas hold.

3 Selecting a surface representation

The derivation in the previous section did not depend on a particular representation of the surface S. However, it implied that for efficient and exact computability of the moments the following properties of the surface patches are desirable.

1. polynomial patches
2. low degree patches
3. few patches
4. simple domains

These properties rule out several otherwise excellent surface representations. For example, S-patches [4] and the recent construction by Hughes and Grimm [9] are rational and of high degree so that integrals are best evaluated by numerical approximation. Simplex splines [8] use a large number of pieces and generalized subdivision surfaces, e.g. [5] [1] [22], lack a global analytic definition for application of the divergence theorem (see however [17]). While nonlinearly-trimmed NURBS patches violate the simple domain requirement, standard polynomial tensor-product B-splines as well as [23], [20], [18], match the requirements, but are of higher degree and hence more expensive to evaluate than C^1-surface splines [15]. In the following sections, we will use piecewise cubic surface splines for the experiments, not in the least because they allow interactive modeling of smooth and non-smooth surfaces of arbitrary patch layout and topological genus. The appendix has a synopsis of surface spline properties and the corresponding surfacing algorithm.

4 Computing surface integrals

To determine the moments, integrals of type

$$\int_U x^i y^j z^k n_3 \, dudv$$

are evaluated. For example, for cubic patches, the integrands of the qth moment are scalar-valued polynomial pieces in two variables and of total degree

$$d = 3(q + 1) + 4,$$

i.e. degree 7, 10 and 13 respectively for the first three moments. The exact integral of a piece is simply the average of its Bernstein-Bézier control points (see e.g. [3]); that is integration consists of summing $k := (d + 2)(d + 1)/2$ coefficients and dividing by k.

To verify that the moment calculation fits into an interactive environment, we compute the *number of operations*. The polynomial n_3 is the difference of products of derivatives. Algorithms for differentiation and multiplication of polynomials in the Bernstein-Bézier form are standard and can be found in many text books, e.g. [7] and in the short article [3]. For the count we recall that a polynomial of degree d in two variables has

$$\mu(d) := \binom{d+2}{2}$$

coefficients.

- Differentiation requires $\mu(d - 1)$ differences.
- Integration requires $\mu(d)$ additions and one division.
- Multiplication of two scalar-valued polynomials of degree d_1 and d_2 respectively, requires $\mu(d_1)\mu(d_2)$ multiplications and $\mu(d_1)\mu(d_2) - \mu(d_1 + d_2)$ additions provided we prescale and postscale the coefficients with precomputed binomial multipliers $\binom{d_j}{i}$ at a cost of $\mu(d_1) + \mu(d_2) + \mu(d_1 + d_2)$ multiplications.

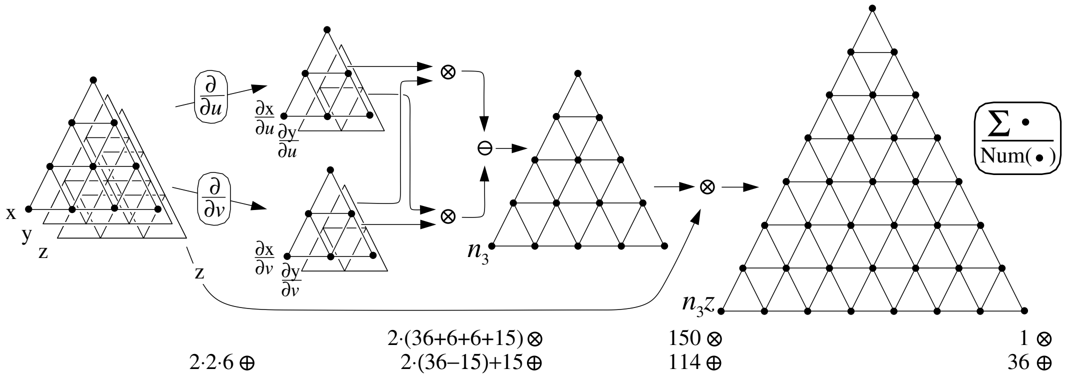

Figure 1: Computing schema for the volume contribution of a cubic Bézier patch.

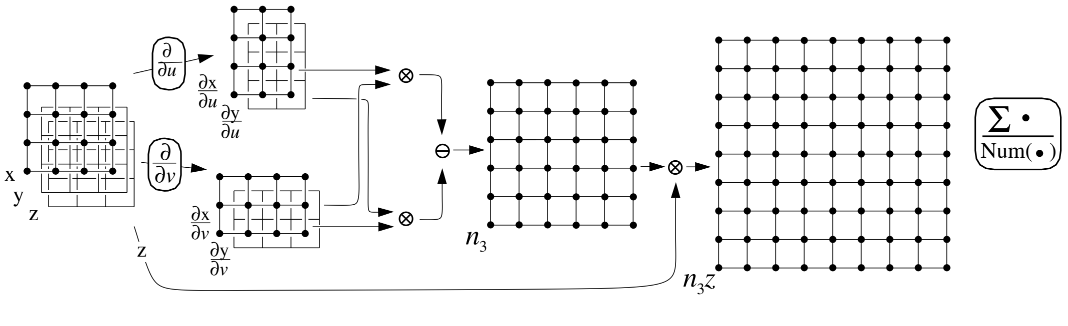

Figure 2: Computing schema of the volume contribution of a bicubic Bézier patch.

Figure 1 depicts the computation of the volume contribution of a cubic patch together with the corresponding operation count: there are four differentiations at $6\oplus$ each, two multiplications at $(36+6+6+15)\otimes$ and $(36-15)\oplus$ each, the addition of two degree 4 scalar-valued polynomials at $\mu(4)\oplus = 15\oplus$ and the final multiplication of a degree 4 with a degree 3 polynomial. The additional work for each moment is tabulated below. The work includes pre- and postscaling which is not necessary when the polynomials are reused in further calculations since the prescaling of the next undoes the postscaling. Figure 2 shows the same process for a bicubic patch.

moment	d	$+$	$\cdot$
n_3	4	81	126
volume	7	114+36	211
centroid	10	$(294+66)\cdot 3$	$436 \cdot 3$
inertia	13	$(660+105)\cdot 6$	$775 \cdot 6$

Hence, we can compute the volume contribution of one patch in roughly 570 operations and all components of the first three moments of a patch in less than 12K operations.

5 Measuring Moments

The principal inertia directions are axes of symmetry with respect to mass distribution and are computed as eigenvectors of the inertia tensor $\mathcal{I}$. The eigenvalues of the inertia tensor represent resistance to torque. Both sets of information are displayed in the inertia frame, a stencil attached to the center of mass whose legs are aligned with the principal inertia directions and stretched according to the corresponding eigenvalues. The smoothed brick shape in Figure 3 is displayed to provide a simple example of an inertia frame. Figure 4 shows three snapshots of a real time design sequence that modifies the geometry of the brick. More complicated objects are shown in Figure 5. In Figure 5(*top*), the geometry of the object is changed by moving one arm of the robot gripper, the result of lifting the surface spline control net. In Figure 5(*bottom*), the geometry of the object is changed by smoothing, the result of changing the surface spline cut ratios from zero to 0.5. The shadow is generated

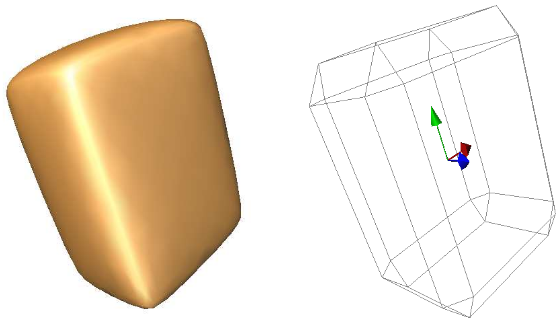

Figure 3: The inertia frame of a smoothed brick shape. The inertia frame is formed by the principle directions of the inertia tensor attached to the center of mass.

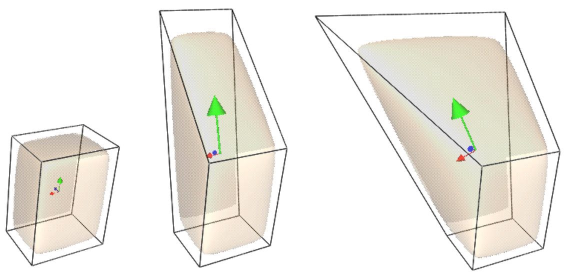

Figure 4: Change of the inertia frame under distortion of the transparently rendered brick.